ANNUAL REVIEWS

Annual Review of Control, Robotics, and Autonomous Systems

Control as an Enabler for Electrified Mobility

Andrew G. Alleyne and Christopher T. Aksland

Department of Mechanical Science and Engineering, University of Illinois Urbana-Champaign, Urbana, Illinois, USA; email: alleyne@illinois.edu

Annu. Rev. Control Robot. Auton. Syst. 2022. 5:659–88

First published as a Review in Advance on October 13, 2021

The *Annual Review of Control, Robotics, and Autonomous Systems* is online at control.annualreviews.org

https://doi.org/10.1146/annurev-control-042920-012513

Keywords

electrified mobility, multidomain modeling, graph-based modeling, hierarchical control

Abstract

This article outlines the importance of electrified mobility (e-mobility) in modern transport. One key goal of this review is to illustrate the role that control has played, and must continue to play, as e-mobility grows. The coordination of power in multiple modes (mechanical, electrical, and thermal) requires sophisticated controller algorithms. This review advocates for model-based approaches to control since there may not be readily available physical systems from which to gather data and do data-based control. A second goal of the article is to present methods for modeling these powertrain systems that are modular, scalable, flexible, and computationally efficient. A graph-based approach satisfies many of the desired criteria. The third goal is to review control approaches for these classes of systems and detail a hierarchical approach that makes trades across different domains of power. Optimization-based approaches are well suited to achieving the regulation and tracking goals, along with the minimization of costs and the satisfaction of constraints. Multiple examples, within this article and the references therein, support the presentation throughout. This field of e-mobility is rapidly growing, and control engineers are uniquely positioned to have an impact and lead many of the critical developments.

1. INTRODUCTION AND MOTIVATION

There is a current acceleration in electrified mobility (e-mobility), building off steady increases in its prevalence and performance in various market sectors over the past several decades. In commercial use, we now see greater numbers of electrified vehicles and greater use of electricity per vehicle, including complete electrification. This growth trend spans all domains of mobility—from automobiles, to aircraft, to ships, to trains, and even to personal transport. As described by Sovacool (1), the typical timescale for a transition in energy technologies is on the order of decades. A major hurdle of this transition is the entrenched infrastructure, which consists of significant capital that supports incumbent technologies and slows the pace of any transition. As such, it is reasonable that e-mobility would take decades to grow from nascent to a significant portion of the overall mobility portfolio. The key variable is the gradient of market penetration over a prolonged duration. As shown below, the interest and research investment in creating the market have been prevalent for at least two decades and span multiple mobility modes. In this sense, e-mobility is here to stay and, frankly, is rapidly reaching a tipping point. The rest of this section briefly highlights the breadth of e-mobility efforts across automotive, aviation, and marine markets and then outlines the rest of the article.

In 2007, Chan (2) published an excellent review that covered the background and history of automotive on-highway electric vehicles and hybrid electric vehicles. This paper illustrated the early tail of the electrification push, when much of the technology was being developed and the right market was being sought. At the start of the twenty-first century, there were still several open research questions surrounding the architecture (parallel, series, or power split), the storage technology, the motor technology, and other aspects. In addition to discussing the energy storage and the powertrain architecture, Chan (2) also illustrated some of the early control algorithms used to govern power flow. There has been a steady increase in research activity in the modeling and control of these systems (3, 4). In most estimates, the compounded annual growth rate of electric passenger vehicles is projected to be in the 10–20% range globally throughout the 2020s, which further emphasizes the current and future impact.

The growth trends associated with on-highway vehicles can also be seen in the aerospace sector. A study by the National Academies of Sciences, Engineering, and Medicine (5) described the long-standing challenges and drivers pushing reduced carbon emissions from the aerospace sector. Aircraft electrification bypasses some of the inefficiencies inherent in bleed-air actuation for vehicle components, thereby reducing fuel burn and carbon emissions. Replacing pneumatics with generators and electrical distribution gained efficiency and flexibility, albeit with some new technical challenges, such as thermal management. Gnadt et al. (6) provided a good overview of efficiency and environmental motivations for both more electric aircraft (MEAs) and fully electric aircraft. In addition to the National Academies study (5), Wheeler & Bozhko (7) discussed power distribution within MEAs and detailed the resulting fuel burn and emissions. As in the automotive domain, the evolution of MEAs has been decades in the making, with a steady increase in the level of power moving through each generation of commercial and military aircraft (8, 9). Madonna et al. (10) discussed the long-term trend of increases in electrification for this mode of mobility. Brelje & Martins (11) and Cano et al. (12) described the wide variety of architectures available for optimizing MEA performance for fixed-wing aircraft, illustrating that there is still much to be done in optimizing electrified powertrains for aircraft. Additionally, several reviews and overviews have provided further details on electrified aircraft, including efforts in power generation and distribution technologies (10, 13, 14). Madonna et al. (10) illustrated the increased level of electrical power used in each new generation of aircraft. For fully electric aircraft, the propulsion must come from electric machines—either large ducted fans or distributed motors, such as those proposed in NASA's X-57 Maxwell program. Ni et al. (13) and Cao et al. (14) highlighted the various generators, motors, and drive topologies most relevant to electrified aircraft.

The same trends as in cars and aircraft can be seen in ships as well. Doerry et al. (15) outlined the history of electric ship propulsion and integrated power systems for the US Navy, including the explicit establishment of its Electric Ships Office in 2007. Much like the cars and aircraft, increased efficiency and range were strong initial motivators, along with environmental impact. For example, Nguyen et al. (16) illustrated how the electrification of marine systems is a key enabler for managing CO_2 emissions in shipping. Additionally, Geertsma et al. (17) described ship power and propulsion systems and then showed that smart ships, combining both electrification and control, can reduce fuel consumption by 10–35%. The electrification of ship systems also allows for advanced electric propulsion systems to be deployed that do not require a mechanical connection between the prime mover engine and the ship's propellers, which gives a great deal of flexibility in ship designs and interior layouts. The ABB Azipod system (18) is one example of an advanced electric propulsion system that provides improved cargo space and reduced componentry by eliminating shafts, steering, and rudder subsystems, all while consuming less power, generating less noise, and providing better maneuverability.

The long-term trends given above for the automotive, aviation, and marine domains can also be seen in buses, trucks, trains, and all other modes of transport, including those in agriculture and construction (19). This is a large opportunity for controls contributions since control is a key enabler for all e-mobility. The goals of this article are threefold. The first is to highlight the importance of e-mobility and illustrate the critical role that control plays. Since these systems are complex, with interconnected dynamics, the effectiveness of their control is essential to their efficiency and performance. The second goal is to discuss the appropriate modeling approaches for model-based control. The approaches must capture the behavior of dynamical systems spanning multiple timescales and multiple physical domains, and we introduce a particular approach that is useful for this problem class. The third goal is to introduce a model-based approach for the control of the complex mechanical–chemical–electrical–thermal systems that make up the electrified powertrains for various mobility applications. Here, we advocate for a hierarchical control approach.

This section, along with the references therein, has demonstrated the importance and scope of the problem. The rest of this article discusses the controllers that enable electrification to occur. Section 2 defines the elements of the control problem, thereby illustrating the role of control in e-mobility. Section 3 presents models and modeling approaches necessary to implement model-based control, along with a brief justification for the use of model-based approaches. Section 4 develops optimization-based controllers for these systems and introduces a particular hierarchical control approach that is well suited to the problem. This section also provides a stability analysis for the presented architecture that builds on the system representations in Section 3. A conclusion then summarizes the main points of the article.

2. ELECTRIFIED MOBILITY AND CONTROL

Within e-mobility, control plays a key enabling role since it coordinates the flow of power among multiple subsystems. As shown conceptually in **Figure 1** for an exemplar on-highway vehicle powertrain, these subsystems can comprise combustion, energy storage, power generation, power conversion and distribution, and load applications. The critical subsystems also include the thermal management that prevents electronic systems failure. Controllers for coordinating these interactions, as illustrated in **Figure 1**, are necessary for a safely functioning vehicle. Power can flow in the mechanical, chemical, electrical, or thermal domains. Similarly, control decisions can be made within each domain, as illustrated in **Figure 1** with separate controllers. These individual

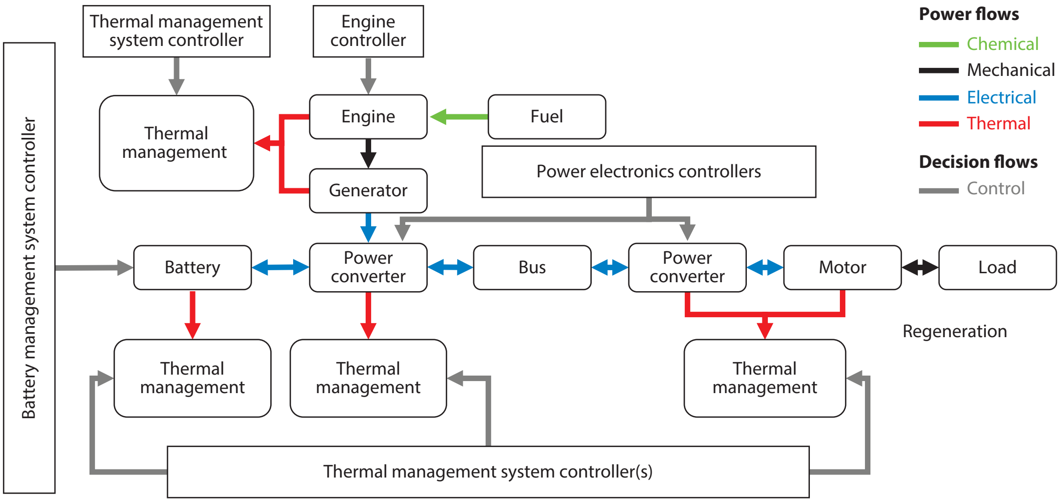

Figure 1

Multidomain power flow and controllers within a simplified version of a candidate on-highway vehicle. The arrows show flow of power in different physical domains. There are multiple components that connect to make a functioning powertrain, which can be complex.

controllers are also on a network, allowing potential coordination among controllers. The goals of the overall control system are to meet power demands as completely and efficiently as possible while observing system constraints. The rest of this section discusses power flow components such as those found in **Figure 1** and then elaborates on the goals for control.

For the vast majority of e-mobility platforms, electricity is stored in batteries. Battery energy density and charging rates are seen as the two largest hurdles for e-mobility. Andwari et al. (20) reviewed a range of battery chemistries for on-highway vehicles along with their costs, energy density, and relative commercial readiness. They also detailed their projected performance and costs based on information from multiple sources. Lithium-ion batteries and their variants, which have an energy density of 100 to more than 250 Wh/kg, are the proposed workhorse for e-mobility in the foreseeable future.

Electrical generation and load applications can be thought of as analogs of each other: One converts mechanical power to electrical power, and the other converts electrical power to mechanical power. These applications are electrical machines that are termed generators or motors depending on their use. Madonna et al. (10) described a variety of machines used on aircraft for generating electricity, including systems driven pneumatically from bleed air and systems driven through a gearbox from a turbo-fan spool shaft. Zhang et al. (21) detailed a variety of architectures and reviewed different metrics for electric motors that could be used in aircraft propulsion, including permanent magnet synchronous machines, induction machines, switched reluctance machines, and wound-field synchronous machines. In automotive applications, AC machines are common, including induction machines and, as found in the Tesla Model 3, synchronous reluctance machines.

Electrical power distribution is critical in larger applications, where the distances to transmit the power are relatively long and the power levels are relatively high. Specific domains include ship systems and aircraft. Several papers have provided overviews of various architectures for power distribution in MEAs (10, 13, 22) and power distribution systems on larger ships (16, 17). Both ships and aircraft utilize multiple generator systems, with commercial aircraft typically having two engines and an auxiliary power unit. One major difference is the power levels, with

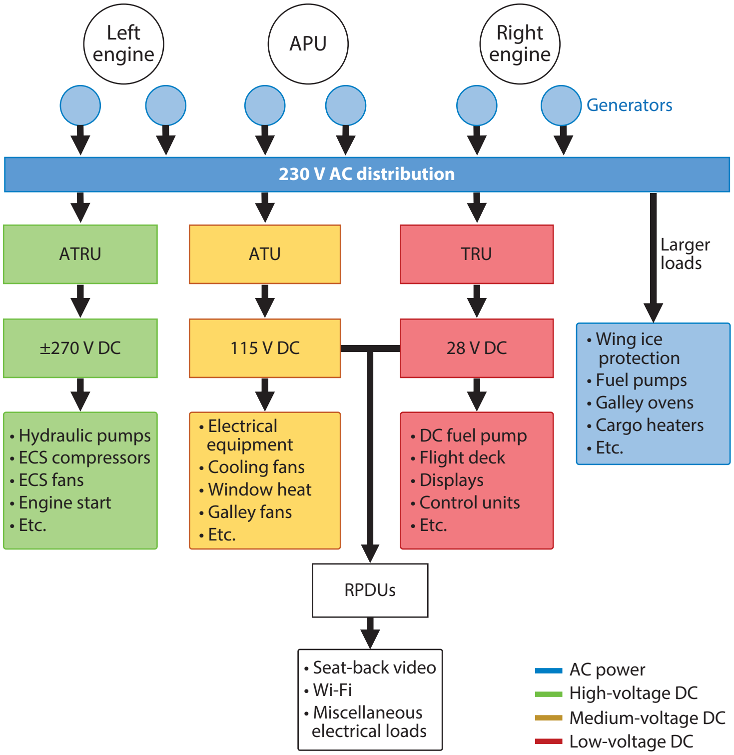

Figure 2

Schematic overview of an MEA power distribution system, showing a hierarchical structure and multiple electrical power levels. Abbreviations: APU, auxiliary power unit; ATRU, auto-transformer rectifier unit; ATU, auto-transformer unit; ECS, environmental control system; MEA, more electric aircraft; RPDU, remote power distribution unit; TRU, transformer rectifier unit. Figure adapted from Madonna et al. (10) with permission; copyright 2018 IEEE.

medium-voltage DC distribution on ships having kilovolts in power ratings, whereas aircraft are typically limited to ±270 V DC to avoid corona discharge effects. For both, there are multiple voltage levels and, typically, conversions between AC and DC.

Converting the power in e-mobility systems requires power electronics such as buck–boost converters, inverters, and rectifiers. These components are at the heart of e-mobility systems since much of the intelligence is embedded there. Details of these types of power electronics can encompass switching frequencies, semiconductor bandgap material, and various architectures. However, for the purposes of this work, we consider the average-value behavior of the power electronics, as detailed in the modeling efforts in Section 3. **Figure 2** shows a schematic of the power distribution system used onboard the Boeing 787 aircraft. As shown, there is a multilevel hierarchy of power flowing down from the main generation units to different power components operating at different levels and power types.

A key element in many e-mobility power systems is the thermal management necessary to keep all electronic components within temperature bounds. Left out of **Figure 2** are the fuel and thermal management systems that are critical to the overall system performance. These systems also fit into a hierarchical format, with primary heat rejection systems being fed by lower-level systems. As electricity flows, it generates heat through resistive losses. Bandhauer

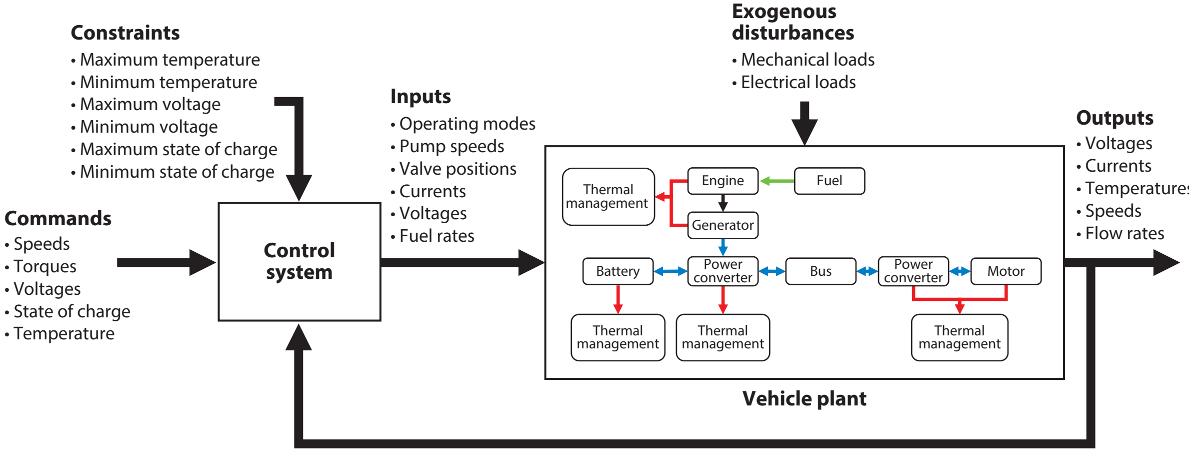

Figure 3

Schematic overview of the e-mobility control problem. The controller manages a multivariable complex system and seeks to achieve commanded responses while observing system constraints. The overall control problem comprises subproblems that incorporate reference trajectory tracking as well as setpoint regulation.

et al. (23) provided a thorough review of thermal management issue for batteries, specifically lithium-ion batteries, which should be kept between approximately 20°C and 40°C for peak operating efficiency and lifetime. Similarly, most silicon-based power electronic systems should stay below 125°C to help maintain reliability. Excessive electric machine temperatures can reduce efficiency and eventually lead to failures, such as winding insulation breakdowns that then lead to short circuits. There are several approaches to thermal management, including heat sinks and exchangers, conductive filler materials, phase change materials, and various types of air and liquid cooling systems operated by free or forced convection.

Coordinating the flow of power among the previously described subsystems to meet a specific demand is the role of the controller. **Figure 3** shows a simplified schematic of the e-mobility control problem under study, with **Figure 1** as the example plant. Here, the controllers illustrated in **Figure 1** are assumed to be aggregated and coordinated in one control system block. Not shown is any estimation that is necessary to extract information for controller usage but can be readily incorporated. It should be noted that some systems can have many electrical loads, and in some cases the nonpropulsive electrical load can be of the same magnitude as the propulsive load. The control system determines mechanical, electrical, and thermal system inputs to send to the subsystems in order to meet the demands of the operator or a higher-level vehicle controller. Simultaneously, it must respect constraints such as battery minimum/maximum state of charge or component temperature limits. The control must also switch between operating modes since not all modes of power flow within the system need be active at all times (e.g., regeneration versus active power production). Interestingly, the control task is simultaneously one of both regulation and tracking under constraints. Regulation problems occur, for example, in maintaining power quality (voltage) on a bus independent of current flows onto and off the bus. Tracking problems occur, for example, if an output vehicle speed profile is commanded.

The performance of the control system is often judged by three elements. First is effectiveness or performance, which is the ability to achieve the commanded values, in either regulation or tracking. Next is energy usage, which is the amount of energy taken to achieve a particular set of tasks over some time horizon. This energy usage can also be compared with that of a baseline controller to determine relative efficiency improvements. Additionally, this metric can also be energy used per unit of output achieved (e.g., distance traveled). Third is safety or reliability, which is often captured in the observation of constraints. These three elements can be seen in the following equations:

$$\text{Performance}: L_{\text{performance}} \triangleq \|\mathbf{x}_{\mathbf{desired}} - \mathbf{x}\|, \tag{1}$$

$$\text{Energy usage}: L_{\text{energy}} \triangleq \int_{t_0}^{t_{\text{final}}} (\text{net power})\text{d}t, \tag{2}$$

$$\text{Safety or reliablity}: L_{\text{reliability}} \triangleq \left\| \text{sat}\left(\left\{\underline{x} - x, x - \bar{x}\right\}\right)_0^\infty \right\|_\infty, \tag{3}$$

where $\mathbf{x}(t)$ is the system state vector, $\mathbf{x}_{\mathbf{desired}}(t)$ is the tracking or regulation reference vector, and $\underline{x}(t)$ and $\bar{x}(t)$ are the minimum and maximum constraints, respectively, on the individual state $x(t)$. The variable $L_{(\cdot)}$ represents a cost used in optimization. The norms can vary depending on the particular metric of interest; for example, for safety the maximum deviation from a constraint may be more important in some cases than the duration of time spent violating the constraint, and for other cases the reverse may be true. Although other metrics can be utilized to evaluate the controller effectiveness, these three are often a foundation for the control problem.

Controllers for e-mobility date back to the early stages of e-mobility since control was a necessary condition for operation. The generalized e-mobility control problem, stated as an optimization problem, is to maximize performance while minimizing energy usage and observing all constraints. Brahma et al. (24) published one of the earliest simulation-based papers looking at dynamic programming for a series hybrid electric car. The system was simplified due to the computational limitations but demonstrated potential for optimization to control electrified powertrains. Lin et al. (25) conducted another early investigation into the optimization of power flow, this time in a parallel hybrid electric vehicle. The controller was initially based on dynamic programming, from which a set of rules was extracted to operate near the behavior of the original dynamic program with more computational efficiency. The objective was to minimize emissions, and this method was an early precursor to online optimal control approaches. Many subsequent efforts in the automotive domain have been similar in approach, with changes to the availability of information or knowledge of the plant.

As indicated above, there are multiple pieces to the overall control problem presented here. Many prior control studies have examined these subproblems without necessarily considering their connections to other aspects; for example, Andwari et al. (20) focused comprehensively on cost and range but did not consider the critical thermal aspects, whereas Bandhauer et al. (23) did the converse. Properly addressing the control problem requires a systems approach that examines the complex interconnections of multiple systems—that is, coordinating the control system block in **Figure 3**. The problem is complicated by its span of multiple physical domains (mechanical, chemical, electrical, and thermal), which means that it also spans a wide range of timescales; for example, the inverter switching dynamics can be on the order of microseconds, while the battery voltage dynamics can be on the order of hours. Williams (9) and Cao et al. (26) provided details on the multi-physics and multi-timescale system representations for aircraft examples. For some vehicles, such as aircraft and ships, the development time is decades, so controllers must be model based because physical prototypes may not exist when the controllers are being developed, verified, and validated. As with any model-based control design, several things are needed: the ability to model the system appropriately, the sensing of relevant variables in the system, a control architecture well suited to the problem framework, and control algorithms derived from the model and the architecture. Since many of the complex vehicles have a hierarchical power flow architecture, as in **Figure 2**, it is natural to consider hierarchical control architectures to match the plant structure. In the following sections, we provide a modeling framework, a hierarchical controller architecture, and algorithms appropriate for complex e-mobility systems.

3. ELECTRIFIED MOBILITY POWER SYSTEM MODELING

The models utilized to describe components for e-mobility systems are many and varied. In this section, we provide an exemplar of dynamic electrical–thermal interaction using a battery model. We then discuss other types of subsystem models that make up the overall system. Due to space limitations, models for all subsystems are not provided, but appropriate references are given. To be effective, the subsystem models should integrate readily into overall system-level models. Various tools and approaches are introduced that can integrate submodels into the overall models. The section concludes with an example of a hybrid electric aircraft system model that uses a graph-based approach.

3.1. Electrothermal Battery Example

As an example, we consider battery systems, which are the primary form of energy storage in e-mobility. In the research domain, battery systems have received the most attention with respect to modeling over the past decade since they are arguably the most challenging components to model properly. Although there are entire fields and journals dedicated to this topic, the focus here is on the elements relevant to system-level integration.

Several papers have provided good overviews of battery models for control-oriented purposes (27–29), including why some of the electrochemical models or partial differential equation models are not suitable for inclusion with, for example, Kalman filters used in determining battery state of charge or state of health. Moura et al. (30) described some of the partial differential equation models as well as equivalent circuit models for batteries. Li et al. (31) reviewed the single-particle model for batteries and augmented it with chemical/mechanical degradation mechanisms. Hu et al. (32) provided a good introduction and explanation of input–output models for batteries, which are often the ones of interest to system integrators. To capture input–output behavior, there are electrochemical models, which fit the partial differential equation type (including single-particle variants), and equivalent circuit models of the ordinary differential equation type. In many cases, particularly away from temperature extremes (e.g., during thermal runaway), the behavior of a battery can be modeled by an equivalent circuit with only resistors and capacitors. **Figure 4** illustrates a second-order equivalent electrical circuit model (33) for a battery cell, which is the most common type in practice.

The electrical system in **Figure 4** can be represented by the voltage dynamics of each of the resistor–capacitor (RC) pairs and the voltage source driving the current flow:

$$C_1 V_1 \dot{V}_1 = -\left(\frac{{V_1}^2}{R_1}\right) + V_1 I_1, \tag{4.}$$

$$C_2 V_2 \dot{V}_2 = -\left(\frac{{V_2}^2}{R_2}\right) + V_2 I_1, \tag{5.}$$

$$Q V_{\mathrm{ocv}} \dot{q} = -V_{\mathrm{ocv}} I_1. \tag{6.}$$

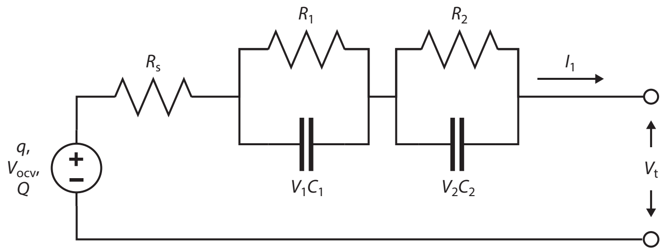

Figure 4

Equivalent circuit model for battery electrical behavior in a cell. A battery's electrical performance is represented as a collection of resistors and capacitors. Figure adapted from Reference 33.

In **Figure 4**, C_1 and C_2 are the electrical capacitance of the capacitors, V_1 and V_2 are the voltages across the capacitors, R_1 and R_2 are the resistances of the resistors in the two RC pairs, R_s is the series internal resistance of the battery, Q is the battery capacity, q is the battery state of charge, $V_{ocv} = f(q)$ is the open circuit voltage, V_t is the cell's terminal voltage, and I_1 is the cell's current demand.

For e-mobility control, it is important for system models to capture the integrated electrical and thermal behaviors. While the thermal load generation of batteries is not as high as that of generators or power electronics, the batteries' performance, health, and durability are strongly affected by temperature. Therefore, models need to be modified to incorporate bidirectional thermal interactions (e.g., as in 33, 34). **Figure 5** illustrates the thermal behavior of a battery cell, which can also be represented using circuit models. The cell temperature dynamics are given by

$$C_c\dot{T}_1 = \underbrace{R_s I_1^2 + \frac{{V_1}^2}{R_1} + \frac{{V_2}^2}{R_2}}_{Q_e} - \frac{1}{R_c}(T_1 - T_2), \tag{7}$$

$$C_s\dot{T}_2 = \frac{1}{R_c}(T_1 - T_2) - \frac{1}{R_u}(T_2 - T_3). \tag{8}$$

In Equations 7 and 8, R_s is again the series internal resistance of the battery, C_c is the heat capacity of the battery core, C_s is the heat capacity of the battery shell, T_1 is the core temperature, T_2 is the surface temperature, T_3 is a surrounding sink temperature, R_c is the internal thermal conduction resistance, and R_u is the thermal convection resistance out to a heat sink. The input thermal

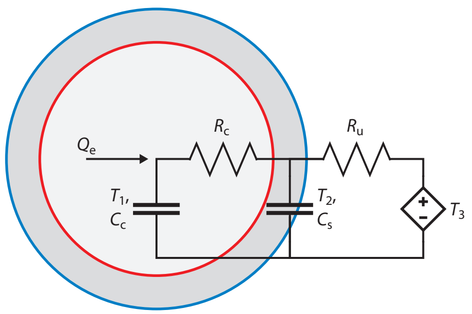

Figure 5

Equivalent circuit model for battery cell thermal behavior. Conduction dynamics and heat transfer are represented by resistors and capacitors to be compatible with the battery's electrical dynamics. Figure adapted from Reference 33.

power is $Q_e = R_s I_1^2 + (V_1^2/R_1) + (V_2^2/R_2)$, which results from the electrical inefficiencies within the cell corresponding to the voltage and current states in the electrical equivalent circuit model in **Figure 5**. The models in Equations 4–8 capture three types of power flow: electrical power (VI), resistive power loss [(V^2/R) and (RI^2)], and conductive thermal transport ($\Delta T/R$). The cell models can be aggregated to create module and pack models as needed.

3.2. Additional Relevant Component Models

Using a battery example, the prior section illustrated the coordination of lumped parameter thermal and electrical component models useful for system-level integration. Other key components can be similarly represented; due to space constraints, only brief expositions are given below, along with references for interested readers to find specific models.

Power electronics do the bulk of power processing and are a key source of heat in the system. The control-oriented electrical models for these systems are static maps since their actual dynamics involve switching in the tens of kilohertz, which is much faster than the other system dynamics (35, 36). They are typically more than 90% efficient in e-mobility systems; however, if the power levels are at the megawatt level, that is still tens of kilowatts of heat that need to be dissipated, usually in a very small volume. Their thermal models (37–39) are much slower, on the order of seconds, and do interact with other timescales in the system.

Electric machines, such as motors and generators, convert between the mechanical and electrical power domains. For hybridized systems, the generators convert mechanical power into electrical AC power that is then put onto the electrical bus for conversion, transport, or storage, as seen in **Figure 2**. Conversely, the motors convert electrical power into mechanical power for motive applications. Most machines for e-mobility are AC induction machines because they have better efficiency characteristics than DC motors. Krause et al. (40) introduced reference frame modeling approaches and direct quadrature modeling of induction machines that allows them to be represented by ordinary differential equations in a manner similar to DC motors. The direct quadrature approach can be used for motors as well as generators (41). Electric machines generate a significant amount of heat within e-mobility systems. Using a finite-element approach, Tikadar et al. (42) provided a comprehensive evaluation of various internal cooling approaches in an electrothermal evaluation of 125-kW permanent magnet synchronous motors for automotive applications. For lower-resolution heat generation models, radially symmetric resistor networks (43) are sufficient to capture thermal dynamics.

Thermal management components couple with the electrical components to enable e-mobility system efficiency, safety, and reliability. For the motor class considered by Tikadar et al. (42), temperature increases can significantly impact efficiency because the motor magnetic properties are temperature dependent. Moreover, Tikadar et al. (42) highlighted the trade-offs inherent in components where improvements in thermal component performance, such as temperature, come at a cost in electrical system performance, such as slot spacing and magnetic flux density. Thermal management not only impacts efficiency and performance but also greatly affects reliability or failure (44). For example, batteries should operate in a relatively narrow temperature range; they should be operated above a lower threshold temperature for efficiency and below an upper threshold temperature for safety and reliability. Bandhauer et al. (23) and Rao & Wang (45) provided good reviews of battery thermal management approaches, including air and liquid cooling as well as phase change materials. Along with the embedded machine cooling approaches detailed by Tikadar et al. (42), other efforts (e.g., 46) have described external cooling approaches for machines that consist of fin design and free or forced convection or advection. These approaches are similar for power electronics cooling. Taken together, the thermal management for batteries, machines, and power electronics constitutes the bulk of thermal management for e-mobility.

3.3. Systems Modeling

Each component that makes up an e-mobility system can incorporate its own modeling approach. Putting multiple components together to create a system means integrating the subsystem models into overall vehicle models. Early efforts at this integration included an article by Powell et al. (47) that outlined hybrid electric vehicle components and gave simple low-order ordinary differential equation representations for motor dynamics, starter/alternator dynamics, battery dynamics, engine dynamics, and vehicle dynamics. While this work was suitable for approximating electromechanical powertrain behavior, improvements in accuracy involved numerical simulation tools based on detailed models appropriate for computer-aided engineering. Examples include the US Department of Energy's Advanced Vehicle Simulator (ADVISOR) systems modeling tool for automobiles (48), which is built in the MATLAB/Simulink software environment, can be used to evaluate electrified cars as well as conventional internal combustion engine cars, and has become well established as a means to replicate system behavior. Langland et al. (49) and Soman et al. (50) introduced a conceptually similar tool within a MATLAB/Simulink framework for representing ship power systems called Smart Ship Systems Design (S3D). S3D was sponsored by the US Navy and its Electric Ship Research and Development Consortium.

Although validated tools are available for ships and automobiles, similar research community tools do not yet exist for aircraft electrified powertrains, largely because electrified aircraft are relatively new. Welstead et al. (51) gave an overview of a NASA tool for Layered and Extensible Aircraft Performance System (LEAPS) development; however, this is more of a static sizing tool than a dynamic simulation tool. Motapon et al. (52) and Lawhorn et al. (53) introduced dynamic systems models for an MEA that included multi-physics dynamic models. The models described by Motapon et al. (52) are taken from the SimPower toolbox as part of the SimScape package in MATLAB/Simulink. Lawhorn et al. (53) used relatively simple differential equations and algebraic relationships; for example, in the electric machine modeling, they introduced both averaged direct quadrature models and switching models for a vehicle similar to the NASA X-57 Maxwell.

A less developed area of systems modeling tools in the literature is the interaction of mechanical, electrical, and thermal subsystems. While Motapon et al. (52) included simple fuel cell models for power generation and Lawhorn et al. (53) included propulsive load models for electrified aircraft, neither presented thermal models or their interaction with the electrical models. A similar gap can be seen in the modeling of electrification for ships and other e-mobility systems. Conversely, Kania et al. (54) initiated dynamic modeling efforts for complex multiphase thermal management systems for future aircraft. McCarthy et al. (55) augmented the work by Kania et al. (54) by adding models of turbomachinery useful for air cycle machines that are also part of aircraft thermal management systems. To fill the gaps in multiple modes of power transfer, a paper by Williams et al. (56) was one of the first in the open literature to develop a dynamic MATLAB/Simulink toolbox that encompassed mechanical, electrical, thermal, hydraulic, and pneumatic domains for aircraft. This tool was used to develop models of more than 10,000 Simulink blocks for vehicles such as the Boeing 737 as well as the Boeing 787 MEA. Cao et al. (26) demonstrated that this toolbox can run faster than real time under certain conditions, making it a good option for hardware-in-the-loop studies or onboard diagnostics.

3.4. General-Purpose Systems Modeling of Power Flow in Electrified Mobility

The modeling and simulation tools discussed above are useful for replicating or predicting system behavior but are not as useful for control design. For control, we need a modeling approach that affords several things. First, the approach should be modular, which allows for various components, possibly from different vendors or with different behaviors, to be swapped without redoing the system simulation. Because e-mobility systems often have multiple design options that must be considered early in the design process, designers need the ability to replace individual components without redoing the rest of the system simulation. A similar motivation occurs when long-lived systems such as aircraft or ships need to have their subsystems upgraded. Second, in addition to being modular, the modeling approach should be scalable—that is, the same modeling approach used for subsystem representation should be usable to represent the connections of subsystems in an overall system. This allows the seamless integration of subsystems to compose larger complex systems. Third, the approach should be flexible, to allow for a mix of multidomain physics-based and data-driven submodels to be easily integrated. Fourth, it should lend itself to analysis tools that can understand the interconnections and aid in model compartmentalization or reduction where necessary. Fifth, while not a technical requirement, it is highly advantageous for the modeling approach to be visually interpretive. Since system-level models are composed of subsystem models, each with its own possible stakeholder, it is good to have an approach that can be easily represented visually so as to allow multidisciplinary teams to understand how and where their subsystems interact. Finally, the models that result from this approach should execute very rapidly and be computationally efficient.

There have been prior efforts to develop general-purpose modeling for systems that manage energy storage and power flow. Stemming from work initiated in electric grid analysis, a paper by Ilic & Jaddivada (57) modeled individual components as state-space models, possibly nonlinear, and then established interconnections among different models, which can take place in a multilayered manner to accommodate different timescales of components. This approach is not particularly scalable since multiple modeling approaches can be used to create the stand-alone models. Additionally, this paper did not describe systems composed of data-driven and model-based components, nor did it highlight visually interpretive tools or those that are readily amenable to network analysis. There have been significant efforts to model and control multi-physics systems using port-Hamiltonian approaches, as described in a review by van der Schaft (58). However, as indicated by Ilic & Jaddivada (57), the approaches described in that review have seen limited use in applications due to the complex conditions sought for feasibility and optimality. Most representations have been relatively simple academic examples.

One of the best-known methods for modeling systems as interconnections of subsystems comes from bond graph modeling (59). This approach was originally developed for fluid power systems, and its concept of using effort and flow variables to model dynamic systems was popular from the 1970s through the 1990s in software packages such as 20-sim (60). Bond graphs have been used previously for e-mobility modeling (e.g., 61–67), but their use has not been widespread for this application. As a graphical approach, bond graphs are easily represented visually, are modular, and can represent linear or nonlinear systems. Most bond graph approaches focus on the creation of a system model, and there is less attention paid to model reduction, timescale separation, or other system-level concerns above and beyond replicating the system physics.

An alternative graphical approach to bond graphs is to use conservation-based graphs to model systems and subsystems (9, 68–72). These graphs use energy conservation to capture power flow among individual components and consist of a set of vertices V and a set of edges E. **Figure 6** shows a simple example with five state vertices. Because components are assembled into a system graph, many sources and sinks of a given component are vertices of adjacent components.

To be more formal, we can generalize **Figure 6**. Let $G = (V, E)$ be an oriented graph that captures the energy storage and power flow throughout a system S. The graph consists of a set of vertices $V = \{v_i : i \in \{1, 2, \ldots, N_v\}\}$ and a set of edges $E = \{e_i : i \in \{1, 2, \ldots, N_e\}\}$. The orientation of each edge e_j represents the positive direction of the associated power P_j from the

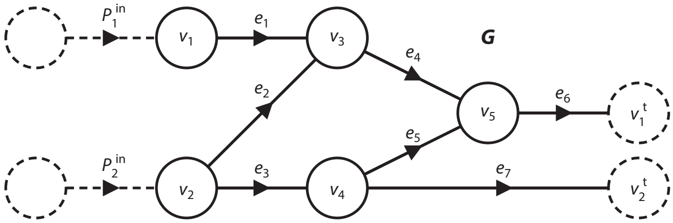

Figure 6

Notional system graph with two input powers and two power sinks. The vertices are the capacitive elements for energy storage, while each edge represents the rate of energy exchange between two vertices, termed power flow. Edges are assigned an orientation, denoted by the directional arrows. Power can also be introduced into the system through external edges labeled P_i^{in} for $i \in \{1, 2\}$. Power can be rejected to external vertices, which are labeled v_i^{t} for $i \in \{1, 2\}$. The dashed circles and dashed edges represent external vertices $V_{\text{t}} \in R^{N_{\text{t}}}$ and external edges $E^{\text{s}} \in R^{N_{\text{s}}}$, respectively.

tail vertex v_j^{tail} to the head vertex v_j^{head}. For the ith vertex, the set of edges directed into the vertex is $E_i^{\text{in}} = \{e_j : v_j^{\text{head}} = v_i\}$, and the set of edges directed out of the vertex is $E_i^{\text{out}} = \{e_j : v_j^{\text{tail}} = v_i\}$. External model interactions are captured by external vertices $V_{\text{t}} \in R^{N_{\text{t}}}$ and external edges $E^{\text{s}} \in R^{N_{\text{s}}}$ (represented in **Figure 6** by the dashed circles and dashed edges, respectively). Let $V_{\text{s}} \in R^{N_{\text{s}}}$ and $V_{\text{t}} \in R^{N_{\text{t}}}$ denote the source and sink vertices, respectively, such that $V_{\text{s}} \subset V$ and $V_{\text{t}} \subset V$. Finally, let $V_{\text{d}} \in R^{N_{\text{d}}}$ denote the N_{d} dynamic vertices such that $V_{\text{d}} \subset V \backslash (V_s \cup V_t)$.

The dynamic state x_i for vertex $v_i \in V_{\text{d}}$ represents the stored energy of that vertex, and the dynamics satisfy conservation of energy:

$$C_i \dot{x}_i = \sum_{e_j \in E_i^{\text{in}}} P_j - \sum_{e_j \in E_i^{\text{out}}} P_j, \qquad 9.$$

where the right-hand side is a summation of all edges oriented into the vertex minus all edges oriented out of the vertex. The power along each edge is constrained to be a function of the adjacent vertex states and an input u_j:

$$P_j = f_j\left(x_j^{\text{tail}}, x_j^{\text{head}}, u_j\right). \qquad 10.$$

The power flow along edges can capture a wide range of memoryless nonlinearities, including nonsmooth ones. The incidence matrix $\mathbf{M} = [m_{ij}] \in R^{(N_{\text{d}}+N_{\text{t}})\times(N_{\text{e}}-N_{\text{s}})}$ captures the structure of the graph and is given by

$$m_{ij} = \begin{Bmatrix} +1 & v_i \text{ is the tail of } e_j \\ -1 & v_i \text{ is the head of } e_j \\ 0 & \text{else} \end{Bmatrix} \qquad 11.$$

and can be partitioned:

$$\mathbf{M} = \begin{bmatrix} \overline{\mathbf{M}} \\ \underline{\mathbf{M}} \end{bmatrix}, \qquad 12.$$

where $\overline{\mathbf{M}} \in R^{N_{\text{d}}\times(N_{\text{e}}-N_{\text{s}})}$ captures the graph structure for V_{d} and $\underline{\mathbf{M}}$ represents how power is flowing to the sink vertices.

The dynamical graph system S can be written as

$$S : \mathbf{C}\dot{\mathbf{x}} = -\overline{M}P + DP^{\text{in}}, \qquad 13.$$

where $\mathbf{C} = \mathrm{diag}([C_i]) \in R^{N_\mathrm{d} \times N_\mathrm{d}}$, $\mathbf{x} = [x_i] \in R^{N_\mathrm{d}}$ represents the states of all dynamic vertices, $\mathbf{P} = [P_i] \in R^{N_\mathrm{e} - N_\mathrm{s}}$ is a vector of each edge power in G that is not from a source vertex, and $\mathbf{P^{in}} = [P_i^{\mathrm{in}}] \in R^{N_\mathrm{s}}$ is a vector of N_s power flows from source vertices. The matrix $\mathbf{D} = [d_{ij}] \in R^{N_\mathrm{d} \times N_\mathrm{s}}$ captures the input of power from the source vertices, and its structure is determined by

$$d_{ij} = \begin{Bmatrix} +1 & v_i \text{ is the head of } P_j^{\mathrm{in}} \\ 0 & \text{else} \end{Bmatrix}. \qquad 14.$$

The vector of edge power flows in S is represented as

$$\mathbf{P} = \mathbf{F}(\mathbf{x}, \mathbf{x^t}, \mathbf{u}) \qquad 15.$$

where $\mathbf{F}(\mathbf{x}, \mathbf{x^t}, \mathbf{u}) = [f_j(x_j^{\mathrm{tail}}, x_j^{\mathrm{head}}, u_j)]$, $j \in [1, N_\mathrm{e} - N_\mathrm{s}]$, resulting in potentially nonlinear dynamics of system S:

$$S : \mathbf{C}\dot{\mathbf{x}} = -\overline{\mathbf{M}}\mathbf{P} + \mathbf{D}\mathbf{P^{in}}. \qquad 16.$$

While the dynamics in Equation 16 can be nonlinear, note that the nonlinearities are all contained in the static functions in Equation 15, whereas the integrators in Equation 9 are linear. This affords a great deal of computational efficiency in numerically simulating the system behavior since integration schemes can process linear behavior more efficiently than nonlinear behavior. In addition, any nonlinear functions of Equation 15 can be linearized, and Equation 16 can be discretized to create linear discrete-time models (as is done in Section 4 for real-time control).

3.5. Graph-Based Multidomain Modeling Example and Validation

The graph-based approach to capturing system behavior is very effective and has been validated across several physical domains. Consider the battery models from **Figures 4** and **5**. A graph model for the coupled electrical–thermal cell is given in **Figure 7** (33). As can be seen, there are three electrical states corresponding to **Figure 4** and Equations 4–6 and two thermal states corresponding to **Figure 5** and Equations 7–8. Reference 33 provides further details for this example.

The modular individual subsystem graphs can be assembled by having the sources of one graph component become sinks for another, which is more intuitive than other approaches, such as bond graphs. **Figure 8** shows a schematic of a hybrid electric unmanned aerial vehicle that

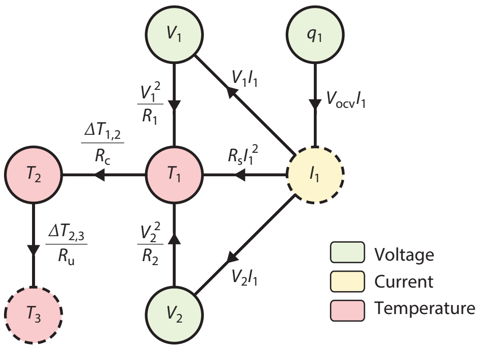

Figure 7

Electrical and thermal graph model for an equivalent circuit battery model. Green indicates voltage energy storage, red indicates thermal energy storage, and yellow indicates current energy storage. Edges represent power flow between adjacent vertices, and the equations for power flow are shown. Figure adapted from Reference 33.

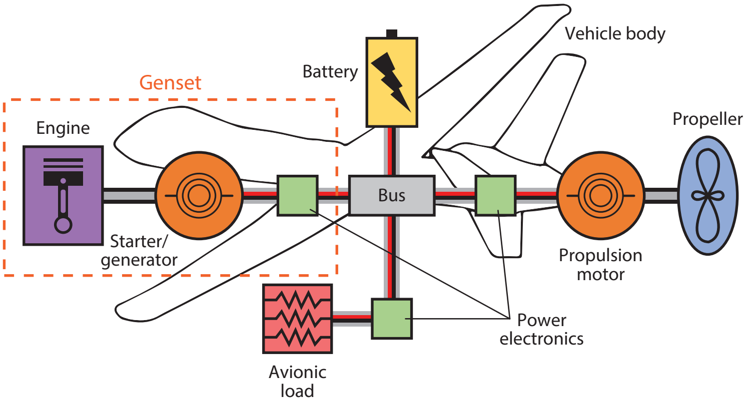

Figure 8

Schematic of a hybrid class 2 unmanned aerial vehicle powertrain consisting of mechanical, chemical, and electrical subsystems. Figure adapted from Reference 33.

consists of mechanical, chemical, and electrical subsystems. Separate models can be developed for each of the components; **Figure 9** shows the combination of multiple labeled subsystems to create an overall system configuration for this vehicle that satisfies the form of Equation 16.

The graph-based approach using integrator-like energy storage elements and potentially nonlinear power flow connections between elements has been demonstrated to be robust and accurate in capturing physical system behavior. **Figure 10** illustrates the validity of this modeling approach, comparing six data streams taken from an unmanned aerial vehicle ground test stand with the outputs of a system model based on **Figure 9**. As can be seen, the approach is very effective. Additional results given by Koeln et al. (68) provided verification and validation of the approach for thermal and hydraulic example systems as well.

3.6. Analysis Tools for Graph-Based Models to Aid Controller Synthesis

Two key challenges in designing controllers for e-mobility systems are their complexity and their multidomain (and hence multi-timescale) dynamics. It is valuable to properly decompose the complex system into smaller subsystems that are interconnected in an architecture amenable to control. In addition to model accuracy and computational efficiency, another key advantage of the graph-based framework for control is the ability to analyze the network of interconnected subsystems. Graphs have been used extensively in control to understand information flow through networks of dynamical systems (73, 74). In the current setting, graph analysis is used to understand physical system behavior, rather than information flow, as well as appropriate representations for controllers.

One key tool is the use of model reduction or model architectures to aid control algorithm synthesis. Multiple techniques can be used for graph-based model reduction. Techniques such as timescale separation (75) have been used to cluster graphs into subsystems with similar timescales; other techniques include minimum-cut methods and spectral methods. There is also a rich literature on additional approaches to decomposing graphs into multiple subgraphs or hierarchies (76), and, as seen in **Figure 2**, a hierarchical representation is a natural one for complex e-mobility power systems. Ji & Geroliminis (77) proposed partitioning based on spatial considerations. Other works (e.g., 76, 78, 79) have used hierarchical clustering approaches, either agglomerative

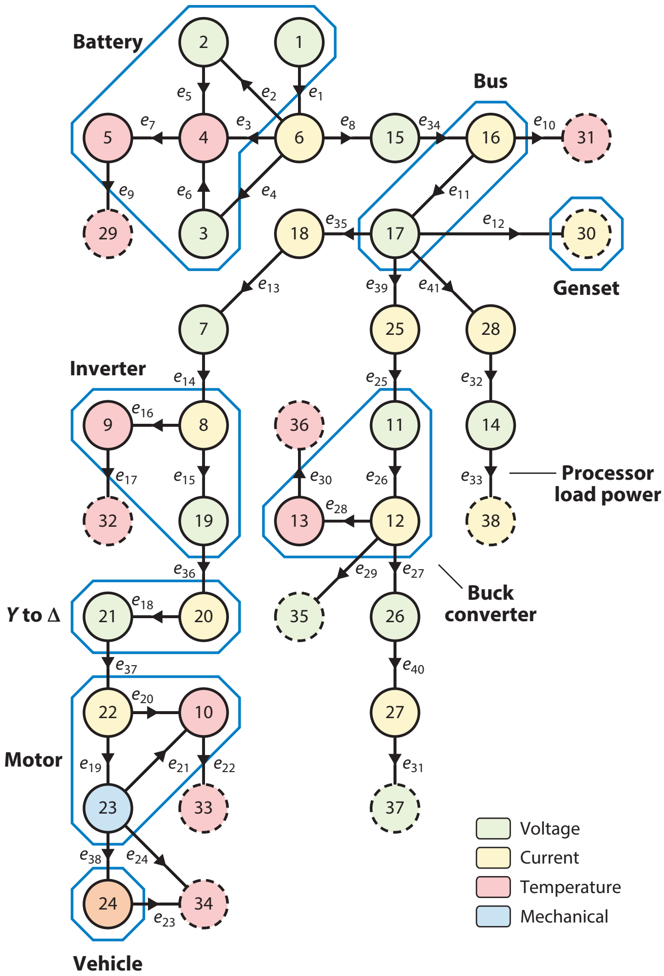

Figure 9

System-level graph model of a hybrid class 2 unmanned aerial vehicle, illustrating separate mechanical, electrical, and thermal component graphs that are interconnected through power flow along edges. Green indicates voltage energy storage, red indicates thermal energy storage, yellow indicates current energy storage, and blue indicates mechanical rotational speed. Dashed circles represent external vertices. Figure adapted from Reference 33.

methods or divisive methods. In agglomerative methods, a user-defined distance metric is calculated for each edge of the graph. Each vertex is defined as its own cluster. For each level of the hierarchy, the closest vertices (i.e., clusters) are merged into subsystems. This is repeated until the graph of the entire system is reconstructed at the top level of the hierarchy. The number of levels in the hierarchy is defined by the user. Divisive clustering approaches progress in an opposite direction. In these approaches, the user starts with the entire graph at the top level of the hierarchy, and as the level of the hierarchy decreases, edges are gradually cut to form smaller subgraphs. However, divisive hierarchical clustering may be NP-hard for large-scale systems (80). At the end of the process, the user is left with a structured model suitable for control. In many cases, the model architecture is hierarchical (as in 76, 78, 79), so that a hierarchical control approach is appropriate.

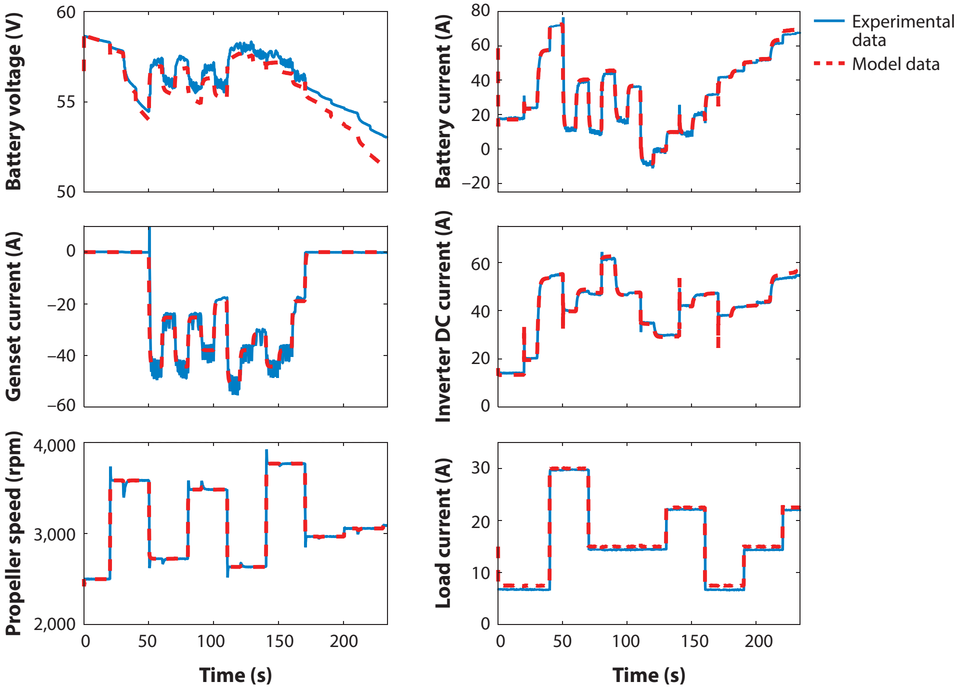

Figure 10

Validation plots for a hybrid class 2 unmanned aerial vehicle model. Figure adapted from Reference 33.

4. CONTROLLER DEVELOPMENT

4.1. Controller Section Overview

As discussed in Section 2, e-mobility controllers have multiple goals. They must provide the demanded power to whatever load requires it. They also must manage the energy storage; provide high-quality power on the electrical buses that transport power, including voltage stability (81, 82); and observe thermal limits, motor torque limits, and other limits. It should be noted that few published e-mobility efforts have explicitly combined the mechanical, electrical, and thermal domains, and most have focused on the electrical or electromechanical domains. The controller goals all lead to a combination of tracking, regulation, and constraint management for the controllers, possibly over multiple physical domains involving widely varying timescales and with dozens of dynamic states. For many systems, this leads to an optimization-based approach to their control.

In the following, we first provide an overview of three optimal approaches that have been used for automotive e-mobility. Second, we present a hierarchical control architecture parallel to the electrical architecture of **Figure 2**. For larger systems, a hierarchical approach, which is a form of distributed control, can be appropriate for dividing a more complex problem into multiple smaller control loops that are more responsive to exogenous signals while still affording a level of centralized planning. Multidomain complex system architectures, such as the example in Section 3.5, naturally lend themselves to a hierarchical representation in timescales (76, 78, 79) and provide efficient control architectures as well. Third, since maintaining stability across interconnected power flow elements is important, we present stability results for the aforementioned hierarchy based on the passivity characteristics of the graph-based models discussed above. Finally, this section concludes with implementation challenges as well as extensions of the results presented in this review.

4.2. Optimal Controller Approaches

There are effectively three groups of optimal controllers used for e-mobility platforms. Dynamic programming is the gold standard in terms of performance but is not implementable since it is not causal and needs to know the whole path ahead of time. The equivalent fuel consumption minimization strategy is another. Model predictive control (MPC), or receding horizon optimization, is a third. We discuss these below but direct readers to References 3, 83, and 84 for further overviews of the different approaches in automotive applications.

The optimal control approach is as follows, where the dynamics are given in the discrete domain since many optimization schemes utilize numerical techniques. Define the system dynamics as

$$\mathbf{x}(k+1) = \mathbf{f}(\mathbf{x}(k), \mathbf{u}(k)) + \mathbf{w}(k),\ \mathbf{x} \in R^{\mathrm{n}}, \mathbf{u} \in R^{\mathrm{m}}, \mathbf{w} \in R^{\mathrm{n}}, \qquad 17.$$

where $\mathbf{x}(k)$ is the vector of states, $\mathbf{u}(k)$ is the vector of inputs, $\mathbf{w}(k)$ is the vector of exogenous disturbances, and $\mathbf{f}(\cdot)$ is a vector representation of the dynamics as a function of states and inputs. Also, define a function J over a horizon N and an instantaneous cost L as a function of the states and inputs:

$$J = \sum_{k=0}^{N-1} L(\mathbf{x}(k), \mathbf{u}(k)). \qquad 18.$$

The goal is to choose an input sequence $\mathbf{u}(k)$ such that J is minimized over the horizon N. This can be augmented by requiring the states and inputs to remain within prescribed sets $\mathbf{x} \in X \subset R^{\mathrm{n}}, \mathbf{u} \in U \subset R^{\mathrm{m}} \forall k \in [0, N-1]$. Furthermore, a terminal cost can be applied to Equation 15:

$$J = \phi\left(\mathbf{x}(N)\right) + \sum_{k=0}^{N-1} L(\mathbf{x}(k), \mathbf{u}(k)). \qquad 19.$$

An example of a terminal cost arises in the charge-sustaining approaches to hybrid electric vehicles, where the goal is to have the battery state of charge be the same at the end of a trip as it was at the beginning. In this case, we could have $\phi(\mathbf{x}(N)) = \mathbf{x}(N) - \mathbf{x}(0)$. Ensuring that $\phi(\cdot) = 0$ is equivalent to a constraint on the final value of a state, in this case the battery state of charge. Sometimes this is done as a soft constraint, where $\phi(\mathbf{x}(N)) = \alpha \|\mathbf{x}(N) - \mathbf{x}(0)\|_2^2$ and α is a factor to weight the constraint versus the rest of the cost function elements. Another example of the terminal cost is the charge-depleting approach, where the goal is to have the battery state of charge at or near its minimum value at the end of a trip. Charge-sustaining approaches are suitable for vehicles that have both chemical fuel energy storage and battery electrical storage.

Early work that applied dynamic programming over a drive cycle included papers by Brahma et al. (24) and Lin et al. (25), which determined the optimal input sequence for the system given in Equation 14 subject to Equation 15 or 16. The dynamic programming is not implementable in real time, so several researchers have sought approximations. Kim et al. (85) introduced a simplified approach based on Pontryagin's minimum principle to approximate the dynamic programming based on a numerical approximation of a Hamiltonian. The simplification allows for efficient real-time computation and implementation. Other approaches, specific to on-highway vehicles, include identifying driving patterns and using a stochastic approach to optimal control (86), then extracting a mapping from system states to control inputs through rules or lookup tables.

The equivalent consumption minimization strategy was originated by Paganelli (87). It is intended for charge-sustaining hybrid electric vehicles and treats the battery as a fuel source, both positive and negative. Any power flowing to or from the battery is equated, through the equivalence factor, to the equivalent amount of fuel that can be saved or used to replenish the battery. The resulting problem is an instantaneous optimization problem, rather than one over a horizon, where the minimum combined electrical and chemical fuel consumption should be minimized (84). The total fuel consumption is

$$\dot{m}_{\text{fuel,equivalent}}(k) = \dot{m}_{\text{fuel}}(k) + \underbrace{\gamma\left(P_{\text{battery}}(k)\right)}_{\substack{\text{conversion of battery}\\ \text{to fuel power}}}, \qquad 20.$$

where γ is a function that converts battery electrical power (in watts) to fuel flow (in grams per second). At every time instant, Equation 20 is used to calculate the equivalent fuel flow for a grid of values for $P_{\text{battery}}(k)$. The value of $P_{\text{battery}}(k)$ returning the lowest value of $\dot{m}_{\text{fuel,equivalent}}(k)$ is then chosen and implemented. There are multiple examples in the literature of implementations of the equivalent consumption minimization strategy (e.g., 88). As outlined by Onori et al. (84) and Serrao et al. (89), the heuristic equivalent consumption minimization strategy can be shown to be equivalent to Pontryagin's minimum principle in the charge-sustaining case and does a very good job of trading off computational complexity for optimality—often closely approximating the optimal solution (90).

Constraints are a key part of any electrified energy management strategy. For storage, there are limits to the charge and discharge rates into and out of the battery. Motors and generators have current limits to them. All electrical systems have thermal limits, which vary depending on the component. For thermal management systems, there are actuation limits in terms of maximum pump rates for liquid cooling systems or fan speeds for air cooling systems. All these limits must be taken into account in the optimization strategy in addition to performance penalties given in Equations 15 and 16. For more complex e-mobility systems, such as aircraft, the balance of constraints with performance makes MPC attractive.

MPC is another optimization approach for e-mobility vehicles where the optimal input sequence is determined over a finite horizon ahead of the current operating condition. The first element of the input sequence is applied and then the optimization problem is resolved. Borhan et al. (91) carried out one of the early implementations of MPC applied to a hybrid electric vehicle, comparing a nonlinear MPC approach with a linear time-varying MPC approach and finding that both of them demonstrated effective energy management. One drawback to MPC approaches is the heavy computational burden, which is often not compatible with the limited computing capability in e-mobility platforms. The general MPC problem solution can be made equivalent to a static, possibly nonlinear, state feedback law (92). Therefore, the solutions can be precomputed as a function of state and stored in lookup tables. This allows for a very efficient and fast MPC implementation, known as explicit MPC, which has been applied in electrified vehicles (92, 93). Another drawback of MPC is that it assumes reasonable knowledge of the desired references and exogenous disturbances during the horizon. For on-highway vehicles, this is challenging, but as vehicles become more connected with the transportation infrastructure, cloud services, and each other, obtaining knowledge of upcoming conditions for energy management becomes more realistic. For other e-mobility platforms—especially larger ones, such as ships and aircraft—their movements are prescribed and constrained by waypoints, and so knowing future exogenous signals is quite feasible.

4.3. Hierarchical Controller Approaches

Many e-mobility systems decompose their control approaches into supervisory high-level control and regulatory low-level control. The high-level systems, often called energy management

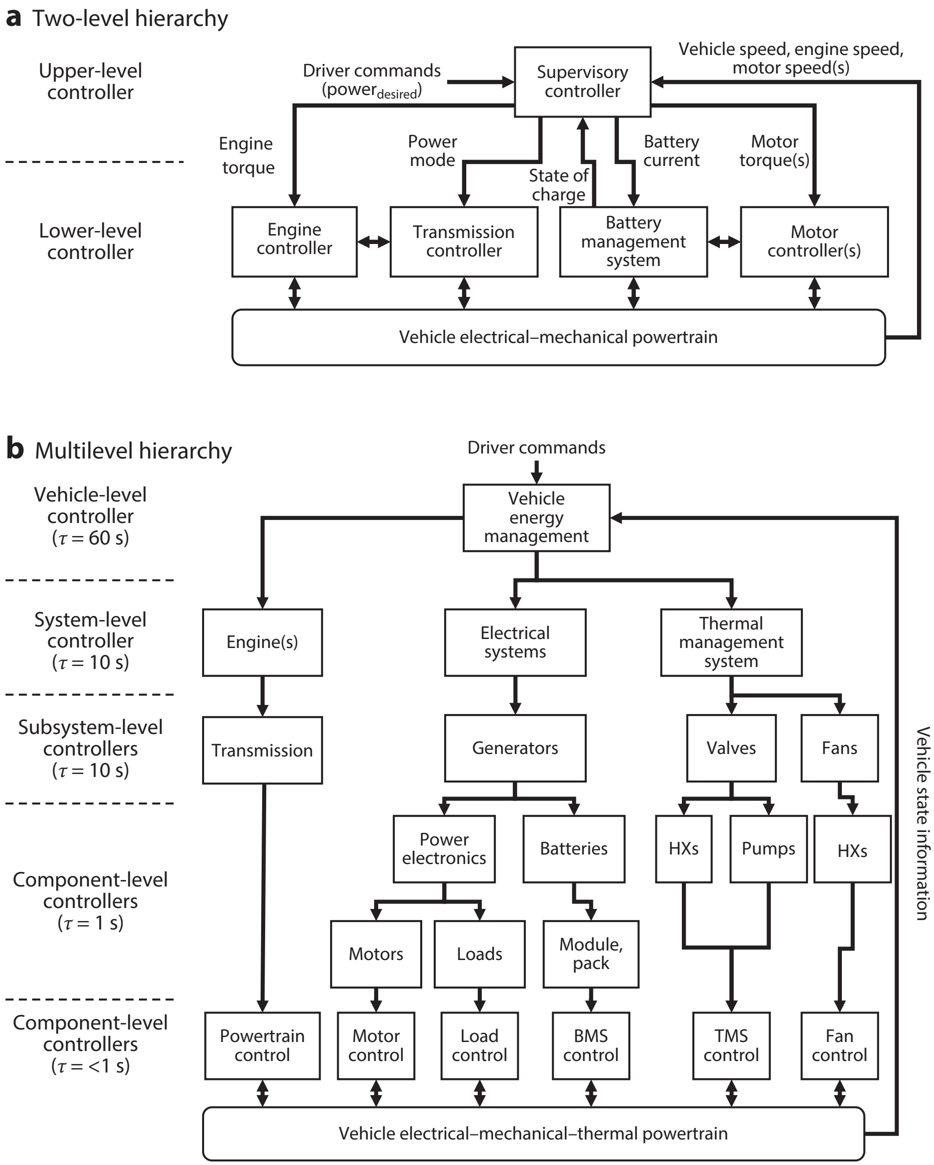

Figure 11

(*a*) Notional two-level supervisory control hierarchy suitable for a hybrid electric passenger vehicle. A relatively simple breakdown of component controllers can be used. (*b*) Notional multilevel hierarchical control suitable for a complex electrified system. Multiple modes of power flow are identified by timescale. Abbreviations: BMS, battery management system; HX, heat exchanger; TMS, thermal management system.

systems, decide the operating mode of the vehicle and send command references to lower-level components. A schematic of such a system is shown notionally in **Figure 11*a***. This approach is appropriate for hybrid electric automotive systems, where the propulsive load dominates other power domains and is the primary focus; however, it can be insufficient in more complex cases, where other loads can be a significant portion of the propulsive load and the thermal loads can be as important as the electrical loads. More complex systems require an integration of multiple domains of power flow, which leads to systems with multiple timescales. A natural extension of the **Figure 11*a*** architecture is given in **Figure 11*b***, which demonstrates multiple timescales represented in a notional multilevel hierarchy.

In **Figure 11*b***, model predictive controllers can be used at the upper levels of the hierarchy to observe system constraints, plan power and energy trajectories, and maximize system performance. The lower levels can be simpler tracking or regulatory controllers to reduce complexity. The decomposition allows the system to react to sudden exogenous signals while looking sufficiently far ahead to avoid constraint violations. This approach affords the benefits of optimization-based controllers with previews while maximizing computational efficiency. Additionally, this approach modularizes the control problem, thereby allowing for component or subsystem changes without reconfiguring the whole algorithm. Several papers have examined various hierarchical architectures for e-mobility subsystems and systems (75, 79, 94). For an example of the use of the hierarchical control approach with an unmanned aerial vehicle, see the sidebar titled Hybrid Electric Unmanned Aerial Vehicle Example along with **Figures 12** and **13**.

4.4. Stability Analysis

Establishing the stability of a system such as the one shown in **Figure 11** is challenging but important since e-mobility systems are safety critical, particularly in aircraft and marine systems. As stated above, the graph-based approach described in Section 3 is useful for decomposing the system into a hierarchy based on the intended use, and several methods of analysis are given in Section 3.3. A variety of results for decomposing electrified vehicle powertrain systems into multi-timescale hierarchies have been published (9, 75, 79). In addition to providing a useful framework for controller design, the graph-based system representation is also very useful for stability analysis of these complex systems. Since systems such as Equation 16 are based on conservation laws, particularly conservation of energy, they can be shown to represent an interconnection of passive dynamic systems (95). If **Figure 6** is the ith subsystem, S_i, in an overall system, with a new variable x_i^{t} representing the states in sink vertices connected to the current subsystem, we can define a set of convenient inputs and outputs as

$$\bar{u}_i = \begin{bmatrix} P_i^{\mathrm{in}} \\ u_i \\ -x_i^{\mathrm{t}} \end{bmatrix} = \begin{cases} \text{power flow into } i\text{th subsystem} \\ \text{actuator inputs} \\ \text{sink states affected by output power flow} \end{cases}, \qquad 21.$$

$$\bar{y}_i = \begin{bmatrix} x_i^{\mathrm{in}} \\ y_i \\ -P_i^{\mathrm{out}} \end{bmatrix} = \begin{cases} \text{internal state affected by inlet power} \\ \text{subsystem outputs} \\ \text{flow out of subsystem} \end{cases}. \qquad 22.$$

Then, defining the storage function (97)

$$V_i = x_i^{\mathrm{T}} C_i x_i \qquad 23.$$

shows that

$$\dot{V}_i \leq \bar{u}_i^{\mathrm{T}} \bar{y}_i \qquad 24.$$

for the ith subsystem, S_i. Furthermore, if multiple subsystems are interconnected such that

$$\begin{aligned} P_{i-1}^{\mathrm{out}} &= P_i^{\mathrm{in}}, \quad x_{i-1}^{\mathrm{t}} = x_i^{\mathrm{in}}, \\ P_i^{\mathrm{out}} &= P_{i+1}^{\mathrm{in}}, \quad x_i^{\mathrm{t}} = x_{i+1}^{\mathrm{in}}, \end{aligned} \qquad 25.$$

HYBRID ELECTRIC UNMANNED AERIAL VEHICLE EXAMPLE

Here, we use the tools presented in this article on a specific example. The system shown schematically in **Figure 8** has a corresponding experimental facility shown in **Figure 12*a***. Utilizing the graph-based models in Section 3, we can construct the model in **Figure 9** and develop a hierarchy based on timescale and functional decomposition. A three-level hierarchical controller for the system is illustrated in **Figure 12*b***. The top level (C_{11}) is an MPC that takes in mission information and manages the battery SOC and load planning. The middle level (C_{31}) is an MPC that performs vehicle reference speed tracking and electrical load following for the avionics and makes decisions about whether the engine is on or off. The lowest-level controllers (R) are proportional–integral regulators that follow the setpoints given by the midlevel controller.

The controller objectives are the same as those defined in Section 2 (Equations 1–3) and include performance, taken as the 2-norm of the state tracking error; reliability, taken as the maximum constraint violation for component states; and efficiency, which considers the total energy consumption over a given mission. A baseline controller (71) utilizing a charge-sustaining policy is implemented for comparison.

Figure 13*a* illustrates a candidate flight load profile in terms of speed and electrical avionic loads for the vehicle (33). At 2,075 s, the avionic loads drop from a mean of 40 A to a mean of 20 A. **Figure 13*b*** shows a comparison between the baseline and hierarchical approaches, with the two lower plots providing a closer evaluation of both the battery and generator currents. When the load drops suddenly, the generator's current production is forced to go into the battery prior to the unloading of the generator. Examining the battery current, one can see that the baseline case exceeds the charging constraint of 10 A on the battery since it is does not properly anticipate the generator being unloaded from 48 A to 40 A. However, the hierarchical approach is able to modify and prepare for the change in load to maintain the maximum battery charge current of 10 A. This clearly improves the reliability metric defined above. Additional comparisons and a demonstration of the efficiency benefits of the hierarchical approach can be found in Reference 33, where fuel usage is reduced by 8–10% for the given mission while achieving similar or better performance.

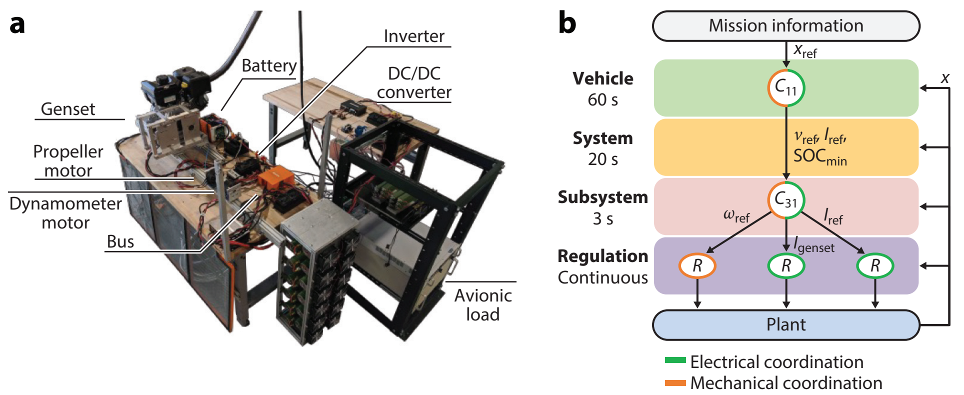

Figure 12

(*a*) Experimental system illustrating the powertrain for a 10-kW class 2 unmanned aerial vehicle. (*b*) A three-level controller hierarchy. Abbreviation: SOC, state of charge.

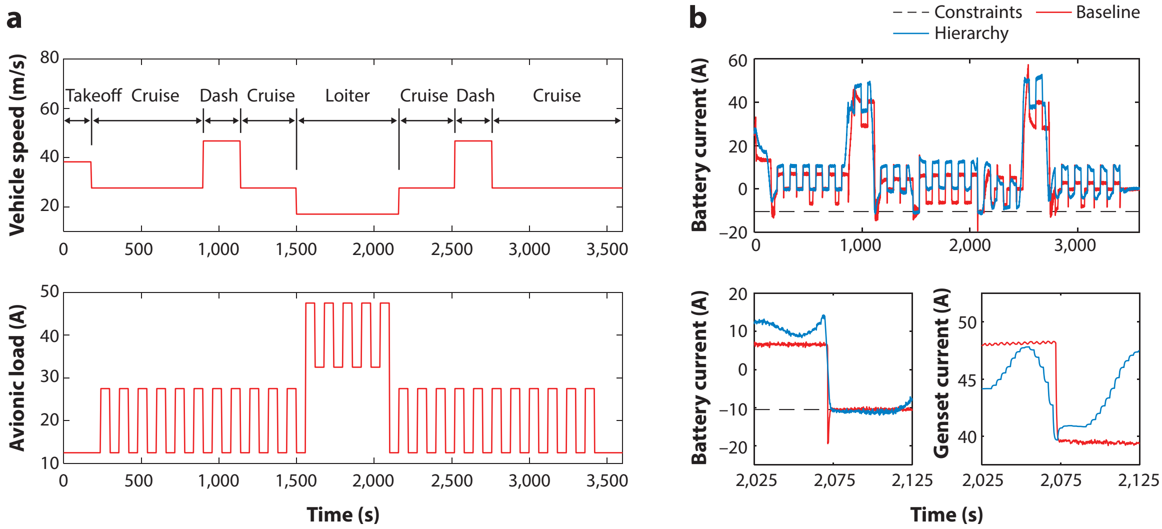

Figure 13

(*a*) Experimental system speed and load profile for a 10-kW class 2 unmanned aerial vehicle. (*b*) Results of the baseline control for battery and generator current.

then their interconnections form an interaction of two passive systems with negative feedback. This interconnection is then passive (95). Concatenating multiple subsystems forms a passive chain or networks, as shown in **Figure 14**.

The benefit is that an MPC controller can be formulated with a constraint to enforce the passivity of the controller interacting with the subsystems. The interconnection of passive subsystems with a negative-feedback interconnection provides a passive overall system that will be stable (97). Since passivity is defined in Equation 24 in continuous time, the MPC formulation given below is also in continuous time. However, the results readily generalize to the discrete

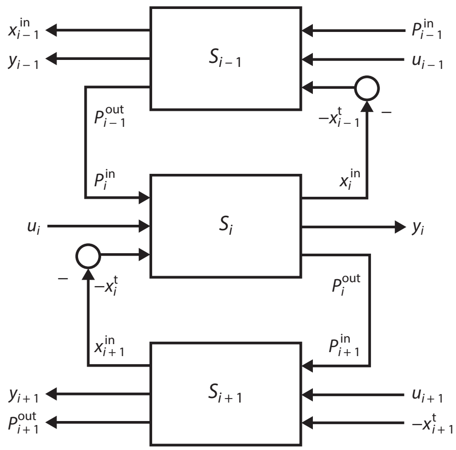

Figure 14

Interconnected passive subsystems forming a passive network. Figure adapted with permission from Reference 96.

time necessary for implementation. Ignoring a terminal cost, the MPC formulation becomes (90)

$$\min_{u_i(\cdot)} \int_0^T L\left(x_i(\tau), u_i(\tau), r_i(\tau), s_i(\tau)\right) \mathrm{d}\tau, \tag{26.}$$

$$\text{subject to } C_i \dot{x}_i = -\bar{M}_i P_i + D_i P_i^{\text{in}}, \tag{27.}$$

$$P_i = f_i\left(x_i^{\text{tail}}, x_i^{\text{head}}, u_i\right), \tag{28.}$$

$$x_i^{\min} - s_i(\tau) \le x_i(\tau) \le x_i^{\max} + s_i(\tau), \tag{29.}$$

$$u_i^{\min} \le u_i(\tau) \le u_i^{\max}, \tag{30.}$$

$$\dot{z}_i = \bar{u}_i^{\mathrm{T}} \bar{y}_i, \quad z_i(\tau) \le \beta_i. \tag{31.}$$

Here, $L(\cdot)$ is the stage cost over the horizon $0 \le t \le T$ and is the continuous-time version of the cost in Equation 18, $r_i(\tau)$ represents the references for each subsystem to track, $s_i(\tau)$ represents slack variables to assist with solution feasibility for the optimization, and the inputs are bounded by $u_i^{\min}$ and $u_i^{\max}$. The function $z_i(\tau)$ is the integral passivity, and β_i is a bound on its overall size. Each ith subsystem need not be passive pointwise in time. As long as the ith controller is sufficiently passive over the horizon, it can violate passivity instantaneously but still result in an overall passive closed-loop system when integrated with the ith plant.

The single-controller configuration given above can be extended to have individual controllers, C_i, on each subsystem, S_i, and these can be networked to create an overall system-level controller. Koeln & Alleyne (97) suggested implementing the approach above at a level of the hierarchy that interacts directly with the plant, such that it is certain that the passive controller is closing the loop with a passive dynamical system.

4.5. Controller Extensions

Several additional aspects of the optimal e-mobility control approaches are practically relevant. In implementation, the hierarchical approach above would be discretized at different sample times depending on the level in the hierarchy. Additionally, the plant dynamics are often linearized about a trajectory so that faster linear MPC can be implemented (72). Additional variations include distributed MPC that is not explicitly hierarchical (94). The distributed MPC in the aircraft example of Reference 94 considers primarily two timescales, engine and electrical, whereas aerospace results from References 71, 75, and 79 demonstrate a hierarchy extension to more than two levels, including engine, electrical, thermal, and hydraulic. Aksland & Alleyne (71) and Koeln et al. (75) validated hierarchical controller performance on two separate aerospace-related hardware-in-the-loop test beds, which included the ability to shed electrical loads to trade off with thermal constraints. Koeln et al. (75) demonstrated that key performance parameters for the hierarchical optimal controller were up to eight times better than those for a baseline controller.

So far, we have assumed the availability of full state information for control, but this may not be the case for large, complex systems. As one example of addressing this challenge, Gomez-Exposito et al. (98) developed a hierarchical estimator based on weighted least squares that was used for smart grid electrical systems that involved one power domain. Tannous & Alleyne (99) extended the concept and developed a multilevel hierarchical estimation framework that matches the hierarchical controller described in **Figure 11*b***, which allows flexibility in handling multiple domains of power and energy by utilizing a heterogeneous mix of estimation schemes. Tannous (100) integrated the multilevel hierarchical estimator with the multilevel hierarchical controller and demonstrated its use in an e-mobility system.

A characteristic of e-mobility systems is their discrete switched modes of operation. The different modes can include or exclude subsystems from the overall system operation. A common example is a hybrid electric automobile functioning with or without the engine engaged. To accommodate the switching among modes, the prior graph topology and resulting system dynamics can be formulated as a switched system (101) and put into a switched hierarchy. Therefore, the prior passivity and MPC controllers can be reformulated in a switched framework (102, 103). This necessitates mixed-integer MPC optimization problems, which can impact computation. Utilizing a quadratic stage cost is one approach to ease the computational burden and make the controller implementable.

A final topic to discuss is fault detection and isolation (FDI). For the graph-based modeling approaches presented, a good FDI architecture is structural analysis (104). Structural analysis follows a similar modular construction as model-based systems to create analytical redundancy relations. This approach affords an architectural advantage in the decomposition of complex systems into simpler systems for individual FDI by appropriate means (e.g., observers). Lukic et al. (105) described an effective use of FDI in an automotive electric vehicle.

5. CONCLUSION

Modern e-mobility systems comprise multiple subsystems that exchange power in various domains: mechanical, chemical, electrical, and thermal. Control is the key enabler that allows these various subsystems to work together and to do so efficiently and safely. The first steps toward controlling these systems are to determine an appropriate framework or architecture with which to develop the control strategy and to choose a modeling approach to complement the architecture. In this article, we advocate a hierarchy that decomposes the overall control problem into simpler subproblems and allows constraints to be imposed across domains. This hierarchy can include two levels, as used in most of the hybrid electric automotive applications, or multiple levels, as illustrated here for more complex systems that need to manage power flow among multiple modes. The next step toward controlling these systems is optimization. The optimization can be determined online or can be found offline and stored in memory for use online. Optimization tools such as MPC, dynamic programming, and other approaches are able to balance the competing demands as well as observe constraints. In a hierarchical setting, different approaches can be deployed at each level of the hierarchy, providing maximum flexibility. Although overlooked in much of the control literature, observing thermal constraints is critical to maintaining the long-term reliability of the vehicle for e-mobility systems.

The model-based approaches are attractive since many vehicles and their systems may not be physically prototyped during controller design. The graph-based approach to system modeling presented here is a promising method for capturing these multidomain systems in a modular and scalable manner. Without sacrificing much in accuracy, the approach affords a significant increase in simulation efficiency, which helps when testing and tuning controllers. The graph-based approach also lends itself to many of the existing graph-theoretic tools that can be used for analysis, such as model reduction or the development of a hierarchical classification.

Although much has been done in the field, there is still room for further contributions. The electrification of mobility is reaching a tipping point, and future systems will be increasingly complex, particularly as increased autonomy and vehicle–vehicle or vehicle–infrastructure coordination are considered. Open research areas at the component level include the interactions of additional physical components, such as fuel cells or hybrid electrical and thermal energy storage elements. At the system level, the open research areas involve the coordination of vehicle-level autonomy with power and energy subsystem autonomy. This is particularly true for groups of interacting vehicles, such as cars on a highway, autonomous construction and mining sites, and swarms of air vehicles. Knowing and coordinating the individual vehicle energy states can impact the overall efficiency of the groups of vehicles. In these and other research topics, the approaches presented here will have a societal impact for decades to come, and control engineers should be leading their development.

DISCLOSURE STATEMENT

The authors are not aware of any affiliations, memberships, funding, or financial holdings that might be perceived as affecting the objectivity of this review.

ACKNOWLEDGMENTS

The authors would like to thank N. Jain, S. Onori, B. Hencey, G. Rizzoni, and M. Williams for their input on this review. The authors' research is supported by the National Science Foundation's Engineering Research Center for Power Optimization of Electro-Thermal Systems (POETS) (cooperative agreement EEC-1449548), the Office of Naval Research (contract N000141912064), and UES (subcontract S-162-11-MR001).

LITERATURE CITED

1. Sovacool BK. 2016. How long will it take? Conceptualizing the temporal dynamics or energy transitions. *Energy Res. Soc. Sci.* 13:202–15
2. Chan CC. 2007. The state of the art of electric, hybrid, and fuel cell vehicles. *Proc. IEEE* 95:704–18
3. Enang W, Bannister C. 2017. Modelling and control of hybrid electric vehicles (a comprehensive review). *Renew. Sustain. Energy Rev.* 74:1210–39
4. Ali AM, Soffker D. 2018. Towards optimal power management of hybrid electric vehicles in real-time: a review on methods, challenges, and state-of-the-art solutions. *Energies* 11:476
5. Natl. Acad. Sci. Eng. Med. 2016. *Commercial Aircraft Propulsion and Energy Systems Research: Reducing Global Carbon Emissions*. Washington, DC: Natl. Acad. Press
6. Gnadt AR, Speth RL, Sabnis JS, Barrett SR. 2019. Technical and environmental assessment of all-electric 180-passenger commercial aircraft. *Prog. Aerosp. Sci.* 105:1–30
7. Wheeler P, Bozhko S. 2014. The more electric aircraft: technology and challenges. *IEEE Electrif. Mag.* 2(4):6–12
8. Alleyne AG. 2018. Power density as the key enabler for electrified mobility. *Polytechnica* 1:10–18
9. Williams MA. 2017. *A framework for the control of electro-thermal aircraft power systems*. PhD Thesis, Univ. Ill. Urbana-Champaign, Urbana, IL
10. Madonna V, Giangrande P, Galea M. 2018. Electrical power generation in aircraft: review, challenges, and opportunities. *IEEE Trans. Transp. Electrif.* 4:646–59
11. Brelje BJ, Martins JRRA. 2019. Electric, hybrid, and turboelectric fixed-wing aircraft: a review of concepts, models, and design approaches. *Prog. Aerosp. Sci.* 104:1–19
12. Cano TC, Castro I, Rodriguez A, Lamar DG, Khalil YF, Albiol-Tendillo L, et al. 2021. Future of electrical aircraft energy power systems: an architecture review. *IEEE Trans. Transp. Electrif.* 7:1915–29
13. Ni K, Liu Y, Mei Z, Wu T, Hu Y, et al. 2019. Electrical and electronic technologies in more-electric aircraft: a review. *IEEE Access* 7:76145–66
14. Cao W, Mecrow BC, Atkinson GJ, Bennett JW, Atkinson DJ. 2012. Overview of electric motor technologies used for more electric aircraft. *IEEE Trans. Ind. Electron.* 59:3523–31
15. Doerry N, Amy J, Krolick C. 2015. History and the status of electric ship propulsion, integrated power systems, and future trends in the U.S. Navy. *Proc. IEEE* 103:2243–51

16. Nguyen HP, Hoang AT, Nizetic S, Nguyen XP, Le AT, et al. 2021. The electric propulsion system as a green solution for management strategy of CO_2 emission in ocean shippping: a comprehensive review. *Int. Trans. Electr. Energy Syst.* 31:e12580
17. Geertsma RD, Negenborn RR, Visser K, Hopman JJ. 2017. Design and control of hybrid power and propulsion systems for smart ships: a review of developments. *Appl. Energy* 194:30–54
18. Nyland M. 2016. *Construction of a hardware-in-the-loop simulator for Azipod control system testing*. MS Thesis, Aalto University, Espoo, Finl.
19. He X, Jiang Y. 2018. Review of hybrid electric systems for construction machinery. *Autom. Constr.* 92:286–96
20. Andwari AM, Pesiridis A, Rajoo S, Martinez-Botas R, Esfahanian V. 2017. A review of battery electric vehicle technology and readiness levels. *Renew. Sustain. Energy Rev.* 78:414–30
21. Zhang X, Bowman CL, O'Connell TC, Haran KS. 2018. Large electric machines for aircraft electric propulsion. *IET Electr. Power Appl.* 12:767–79
22. Sarlioglu B, Morris CT. 2015. More electric aircraft: review, challenges, and opportunities for commercial transport aircraft. *IEEE Trans. Transp. Electrif.* 1:54–64
23. Bandhauer TM, Garimella S, Fuller TF. 2011. A critical review of thermal issues in lithium-ion batteries. *J. Electrochem. Soc.* 158:R1–25
24. Brahma A, Buezennec Y, Rizzoni G. 2000. Optimal energy management in series hybrid electric vehicles. In *2000 American Control Conference*, Vol. 1, pp. 60–64. Piscataway, NJ: IEEE
25. Lin CC, Peng H, Grizzle JG, Kang JM. 2003. Power management strategy for a parallel hybrid electric truck. *IEEE Trans. Control Syst. Technol.* 11:839–49
26. Cao Y, Williams MA, Alleyne AG, Krein PT. 2016. 20x-real time modeling and simulation of more electric aircraft electrical and thermal power systems. In *2016 International Conference on Electrical Systems for Aircraft, Railway, Ship Propulsion and Road Vehicles and International Transportation Electrification Conference*. Piscataway, NJ: IEEE. **https://doi.org/10.1109/ESARS-ITEC.2016.7841416**
27. Plett GL. 2004. Extended Kalman filtering for battery management systems of LiPB-based HEV battery packs: part 2. Modeling and identification. *J. Power Sources* 134:262–76
28. Plett GL. 2004. Extended Kalman filtering for battery management systems of LiPB-based HEV battery packs: part 3. State and parameter estimation. *J. Power Sources* 134:277–92
29. Chaturvedi NA, Klein R, Christensen J, Ahmed J, Kojic A. 2020. Algorithms for advanced battery management systems. *IEEE Control Syst.* 30:49–68
30. Moura S, Stein J, Fathy H. 2013. Battery-health conscious power management in plug-in hybrid electric vehicles via electrochemical modeling and stochastic control. *IEEE Trans. Control Syst. Technol.* 21:679–94
31. Li J, Adewuyi K, Lotfi N, Landers RG, Park J. 2018. A single particle model with chemical/mechanical degradation physics for lithium ion battery State of Health (SOH) estimation. *Appl. Energy* 212:1178–90
32. Hu Y, Yurkovich S, Guezennec Y, Yurkovich B. 2011. Electro-thermal battery model identification for automotive applications. *J. Power Sources* 196:449–57
33. Aksland CT. 2019. *Modular modeling and control of a hybrid unmanned aerial vehicle's powertrain*. MS Thesis, Univ. Ill. Urbana-Champaign, Urbana, IL
34. Rugh JP, Pesaran A, Smith K. 2011. *Electric vehicle battery thermal issues and thermal management techniques*. Paper presented at the SAE Alternative Refrigerant and Systems Efficiency Symposium, Phoenix, AZ, Sept. 27–29
35. Chen Y, Yuan Z, Luo F. 2018. A model-based multi-objective optimization for high efficiency and high power density motor drive inverters for aircraft applications. In *NAECON 2018: IEEE National Aerospace and Electronics Conference*, pp. 36–42. Piscataway, NJ: IEEE
36. Hegazy O, Van Mierlo J, Lataire P. 2012. Analysis, modeling, and implementation of a multidevice interleaved DC/DC converter for fuel cell hybrid electric vehicles. *IEEE Trans. Power Electron.* 27:4445–58
37. Mantooth HA, Heffner AR. 1997. Electro-thermal simulation of an IGBT PWM inverter. *IEEE Trans. Power Electron.* 12:474–84
38. van der Broeck C, Ruppert L, Hinz A, Conrad M, Doncker R. 2018. Spatial electro-thermal modeling and simulation of power electronic modules. *IEEE Trans. Ind. Appl.* 54:404–15

39. Tannous PJ, Peddada SRT, Allison JT, Foulkes T, Pilawa-Podgurski RCN, Alleyne AG. 2017. Dynamic temperature estimation of power electronics systems. In *2017 American Control Conference*, pp. 3463–69. Piscataway, NJ: IEEE
40. Krause PC, Wasynczuk O, Sudhoff SD. 2002. *Analysis of Electric Machinery and Drive Systems*. New York/Piscataway, NJ: Wiley-IEEE. 2nd ed.
41. Tapia A, Tapia G, Ostolaza JX, Saenz JR. 2003. Modeling and control of a wind turbine driven doubly fed induction generator. *IEEE Trans. Energy Convers.* 18:194–204
42. Tikadar A, Johnston D, Kumar N, Joshi Y, Kumar S. 2021. Comparison of electro-thermal performance of advanced cooling techniques for electric vehicle motors. *Appl. Therm. Eng.* 183:116182
43. Yi X, Sanchez R, Haran K, Veres J, Perry A, Ansell P. 2018. Self-pumped air-cooling design for a high-speed high-specific-power motor. In *2018 IEEE Transportation Electrification Conference and Expo*, pp. 274–79. Piscataway, NJ: IEEE
44. Bailey C. 2008. Thermal management technologies for electronic packaging: current capabilities and future challenges for modelling tools. In *2008 10th Electronics Packaging Technology Conference*, pp. 527–32. Piscataway, NJ: IEEE
45. Rao Z, Wang S. 2011. A review of power battery thermal energy management. *Renew. Sustain. Energy Rev.* 15:4554–71
46. Tong W. 2014. *Mechanical Design of Electric Motors*. Boca Raton, FL: Taylor & Francis
47. Powell B, Bailey K, Cikanek S. 1998. Dynamic modeling and control of hybrid electric vehicle powertrain systems. *IEEE Control Syst. Mag.* 18(7):17–33
48. Markel T, Brooker A, Hendricks T, Johnson V, Kelly K, et al. 2002. ADVISOR: a systems analysis tool for advanced vehicle modeling. *J. Power Sources* 110:255–66
49. Langland B, Leonard R, Smart R, Dougal RA. 2015. Modeling and data exchange in a concurrent and collaborative design environment for electric ships. In *2015 IEEE Electric Ship Technologies Symposium*, pp. 388–94. Piscataway, NJ: IEEE
50. Soman R, Steurer MM, Toshon TA, Faruque MO, Cuzner RM. 2017. Size and weight computation of MVDC power equipment in architectures developed using the smart ship systems design environment. *IEEE J. Emerg. Sel. Topics Power Electron.* 5:40–50
51. Welstead JR, Caldwell D, Condotta R, Monroe N. 2018. An overview of the Layered and Extensible Aircraft Performance System (LEAPS) development. In *2018 AIAA Aerospace Sciences Meeting*, pap. 2018-1754. Reston, VA: Am. Inst. Aeronaut. Astronaut.
52. Motapon SN, Dessaint LA, Al-Haddad K. 2014. A comparative study of energy management schemes for a fuel-cell hybrid emergency power system of more-electric aircraft. *IEEE Trans. Ind. Electron.* 61:1320–34
53. Lawhorn D, Rallabandi V, Ionel D. 2019. Electric aircraft system co-simulation including body, propeller, propulsion, and energy storage models. In *2019 IEEE Transportation Electrification Conference and Expo*. Piscataway, NJ: IEEE. **https://doi.org/10.1109/ITEC.2019.8790529**
54. Kania M, Koeln J, Alleyne A, McCarthy K, Wu N, Patnaik S. 2012. *A dynamic modeling toolbox for air vehicle vapor cycle systems*. Tech. Pap. 2012-01-2172, SAE Int., Warrendale, PA
55. McCarthy P, Niedbalski N, McCarthy K, Walters E, Cory J, Patnaik S. 2016. A first principles based approach for dynamic modeling of turbomachinery. *SAE Int. J. Aerosp.* 9:45–61
56. Williams M, Sridharan S, Banerjee S, Mak C, Pauga C, et al. 2015. *PowerFlow: a toolbox for modeling and simulation of aircraft systems*. Tech. Pap. 2015-01-2417, SAE Int., Warrendale, PA
57. Ilic MD, Jaddivada R. 2018. Multi-layered interactive energy space modeling for near-optimal electrification of terrestrial, shipboard and aircraft systems. *Annu. Rev. Control* 45:52–75
58. van der Schaft A. 2020. Port-Hamiltonian modeling for control. *Annu. Rev. Control Robot. Auton. Syst.* 3:393–416
59. Karnopp DC, Margolis DL, Rosenberg RC. 1990. *System Dynamics: A Unified Approach*. New York: Wiley. 2nd ed.
60. Controllab Prod. 2021. Bond graphs. *20-sim.* **https://www.20sim.com/features/model-libraries/bondgraphs**
61. Filippa M, Mi C, Shen J, Stevenson RC. 2005. Modeling of a hybrid electric vehicle powertrain test cell using bond graphs. *IEEE Trans. Veh. Technol.* 54:837–45

62. Gao DW, Mi C, Emadi A. 2007. Modeling and simulation of electric and hybrid vehicles. *Proc. IEEE* 95:729–45
63. Cipek M, Pavkovic D, Petric J. 2013. A control-oriented simulation model of a power-split hybrid electric vehicle. *Appl. Energy* 101:121–33
64. Rizzoni G, Guzzella L, Baumann B. 1999. Unified modeling of hybrid electric vehicle drivetraings. *IEEE/ASME Trans. Mechatron.* 4:246–57
65. Xu Q, Wang P, Chen J, Wen C, Lee MY. 2017. A module-based approach for stability analysis of complex more-electric aircraft power system. *IEEE Trans. Transp. Electrif.* 3:901–19
66. Silva LI, Jaguemont J, De Angelo CH, Boulon L. 2016. Modeling an electric vehicle lithium-ion battery pack considering low temperature behavior. In *2016 IEEE Vehicle Power and Propulsion Conference*. Piscataway, NJ: IEEE. **https://doi.org/10.1109/VPPC.2016.7791727**
67. Song K, Wang Y, An C, Xu H, Ding Y. 2021. Design and validation of energy management strategy for extended-range fuel cell electric vehicle using bond graph method. *Energies* 14:380
68. Koeln JP, Williams MA, Pangborn HC. 2016. Experimental validation of graph-based modeling for thermal fluid power flow systems. In *Proceedings of the ASME 2016 Dynamic Systems and Control Conference*, Vol. 2, pap. V002T21A008. New York: Am. Soc. Mech. Eng.
69. Williams MA, Koeln JP, Pangborn HC, Alleyne AG. 2018. Dynamical graph models of aircraft electrical, thermal, and turbomachinery components. *ASME J. Dyn. Syst. Meas. Control* 140:041013
70. Aksland CT, Bixel TW, Raymond LC, Rottmayer MA, Alleyne AG. 2019. Graph-based electro-mechanical modeling of a hybrid unmanned aerial vehicle for real-time applications. In *2019 American Control Conference*, pp. 4253–59. Piscataway, NJ: IEEE
71. Aksland CT, Alleyne AG. 2020. Experimental model and controller validation for a series hybrid unmanned aerial vehicle. In *2020 American Control Conference*, pp. 4154–60. Piscataway, NJ: IEEE
72. Pangborn HC, Koeln JP, Williams MA, Alleyne AG. 2018. Experimental validation of graph-based hierarchical control for thermal management. *ASME J. Dyn. Syst. Meas. Control* 140:101016
73. Oltafi-Saber R, Fax JA, Murray RM. 2007. Consensus and cooperation in networked multi-agent systems. *Proc. IEEE* 95:215–33
74. Jadbabaie A, Lin J, Morse AS. 2003. Coordination of groups of mobile autonomous agents using nearest neighbor rules. *IEEE Trans. Autom. Control* 48:988–1001
75. Koeln JP, Pangborn HC, Williams MA, Kawamura MA, Alleyne AG. 2019. Hierarchical control of aircraft electro-thermal systems. *IEEE Trans. Control Syst. Technol.* 28:1218–32
76. Yu J, Huang H, Tian S. 2005. Survey of clustering algorithms. *IEEE Trans. Neural Netw.* 16:645–78
77. Ji Y, Geroliminis N. 2012. On the spatial partitioning of urban transportation networks. *Transp. Res. B* 46:1639–56
78. Schaeffer SE. 2007. Graph clustering. *Comput. Sci. Rev.* 1:27–64
79. Docimo DJ, Alleyne AG. 2018. Electro-thermal graph-based modeling for hierarchical control with application to an electric vehicle. In *2018 IEEE Conference on Control Technology and Applications*, pp. 812–19. Piscataway, NJ: IEEE
80. Guenoche A, Hansen P, Jaumard B. 1991. Efficient algorithms for divisive hierarchical clustering with the diameter criterion. *J. Classif.* 8:5–30
81. Riccobono A, Cupelli M, Monti A, Santi E, Roinila T, et al. 2017. Stability of shipboard DC power distribution. *IEEE Electrif. Mag.* 5(3):55–67
82. Emadi A, Kaligh A, Rivetta CH, Williamson GA. 2006. Constant power loads and negative impedance instability in automotive systems: definition, modeling, stability, and control of power electronic converters and motor drives. *IEEE Trans. Veh. Technol.* 55:1112–25
83. Sciarretta A, Guzzella L. 2007. Control of hybrid electric vehicles. *IEEE Control Syst.* 27:60–70
84. Onori S, Serrao L, Rizzoni G. 2016. *Hybrid Electric Vehicles: Energy Management Strategies*. London: Springer
85. Kim N, Cha S, Peng H. 2011. Optimal control of hybrid electric vehicles based on Pontryagin's minimum principle. *IEEE Trans. Control Syst. Technol.* 19:1279–87
86. Moura S, Fathy H, Callaway D, Stein J. 2011. A stochastic optimal control approach for power management in plug-in hybrid electric vehicles. *IEEE Trans. Control Syst. Technol.* 19:545–55

87. Paganelli G. 1999. *Conception et commande d'une chaîne de traction pour véhicule hybride parallèle thermique et électrique*. PhD Thesis, Univ. Valenciennes, Valenciennes, Fr.
88. Sciarretta A, Back M, Guzzella L. 2004. Optimal control of parallel hybrid electric vehicles. *IEEE Trans. Control Syst. Technol.* 12:352–63
89. Serrao L, Onori S, Rizzoni G. 2009. Equivalent consumption minimization strategy as a realization of Pontryagin's minimum principle for HEV control. In *2009 American Control Conference*, pp. 3964–69. Piscataway, NJ: IEEE
90. Pisu P, Rizzoni G. 2007. A comparative study of supervisory control strategies for hybrid electric vehicles. *IEEE Trans. Control Syst. Technol.* 15:506–18
91. Borhan H, Vahidi A, Phillips A, Kuang M, Kolmanovsky I, DiCairano S. 2012. MPC-based energy management of a power-split hybrid electric vehicle. *IEEE Trans. Control Syst. Technol.* 20:593–603
92. Di Cairano S. 2012. An industry perspective on MPC in large volumes applications: potential benefits and open challenges. *IFAC Proc. Vol.* 4(17)5:52–59
93. Li X, Han L, Liu H, Wang W, Xiang C. 2019. Real-time optimal energy management strategy for a dual-mode power-split hybrid electric vehicle based on an explicit model predictive control algorithm. *Energy* 172:1161–78
94. Dunham W, Hencey B, Girard A, Kolmanovsky I. 2020. Distributed model predictive control for more electric aircraft subsystems operating at multiple time scales. *IEEE Trans. Control Syst. Technol.* 28:2177–90
95. Khalil HK. 2015. *Nonlinear Control*. London: Pearson
96. Koeln JP. 2016. *Hierarchical power management in vehicle systems*. PhD Thesis, Univ. Ill. Urbana-Champaign, Urbana, IL
97. Koeln JP, Alleyne AG. 2017. Stability of decentralized model predictive control of graph-based power flow systems via passivity. *Automatica* 82:29–34
98. Gomez-Exposito A, Abur A, de la Villa Jaen A, Gomez-Quiles C. 2011. A multilevel state estimation paradigm for smart grids. *Proc. IEEE* 99:952–76
99. Tannous PJ, Alleyne AG. 2020. Multilevel hierarchical estimation for thermal management systems of electrified vehicles with experimental validation. *ASME J. Dyn. Syst. Meas. Control* 142:111004
100. Tannous PJ. 2020. *Estimation and fault diagnosis for vehicle energy systems*. PhD Thesis, Univ. Ill. Urbana-Champaign, Urbana, IL
101. Liberzon D. 2003. *Switching in Systems and Control*. Boston: Birkhauser
102. Pangborn HC, Koeln JP, Alleyne AG. 2018. Passivity and decentralized MPC of switched graph-based power flow systems. In *2018 Annual American Control Conference*, pp. 198–203. Piscataway, NJ: IEEE
103. Pangborn HC, Alleyne AG. 2019. Cooperativity and hierarchical MPC of state-constrained switched power flow systems. In *2019 American Control Conference*, pp. 4245–52. Piscataway, NJ: IEEE
104. Atkeson A, Kehoe P. 2001. *The transition to a new economy after the second industrial revolution*. Work. Pap. 606, Fed. Reserve Bank Minneap., Minneapolis, MN
105. Lukic M, Hebala A, Giangrande P, Klumpner C, Nuzzo S, et al. 2018. State of the art of electric taxiing systems. In *2018 IEEE International Conference on Electrical Systems for Aircraft, Railway, Ship Propulsion and Road Vehicles and International Transportation Electrification Conference*. Piscataway, NJ: IEEE. **https://doi.org/10.1109/ESARS-ITEC.2018.8607786**